Research and Development Techniques 1: Potentiodynamic Studies of Copper Metal Deposition

Carlos Ponce de Leon and Frank C. Walsh*

Electrochemical Engineering Group, Department of Chemical Engineering, University of Bath, Claverton Down, Bath BA2 7AY, UK.

**For correspondence. E-mail:cescpdla@bath.ac.uk*

Summary – The electrochemistry of copper (II) (I) ions in aqueous chloride solution, at pH 2, is used to demonstrate the application of voltammetry techniques in characterising electrode processes. The electrolyte used is 1.5 M sodium chloride containing 20 to 50 x 10^{-3} M cupric chloride at 20°C, in which both Cu(II) and Cu(I) ions are stable. A platinum rotating disc electrode (RDE, radius 0.365 cm) is used to provide controlled mass transport under laminar flow conditions. Cyclic voltammetry, at a stationary disc electrode, is used to characterise the general electrochemistry. Four current peaks due to reduction of Cu(II) ions to Cu(I) ions, deposition of Cu from Cu(I) ions, anodic stripping of Cu to form Cu(I) ions and oxidation of Cu(I) ions to Cu(II) ions are seen. Analysis of the Cu(II) Cu(I) couple indicates a reversible process. A potential sweep rate experiment allows the diffusion coefficient of Cu(II) ions to be calculated. The anodic stripping peak in the cyclic voltammogram is used to estimate the amount of copper deposited. Reduction of Cu(II) to Cu(I) then to Cu is examined at a range of rotation speeds (150-1870 rpm) using linear sweep voltammetry at the RDE. Mass transport data are obtained in the form of limiting current density as a function of the RDE speed, allowing the diffusion coefficients of Cu(II) and Cu(I) ions to be calculated.

Keywords: anodic stripping voltammetry (ASV), charge transfer control, copper deposition, copper stripping, cupric ions, cuprous ions, cyclic voltammetry (CV), Levich equation, linear sweep voltammetry (LSV), mass transport control, Randles-Sevčik equation, rotating disc electrode (RDE).

INTRODUCTION

Electrodeposition and dissolution reactions of copper involving Cu(II) Cu(I) ions are important to many sectors of industry, including electroplating, electrowinning, marine corrosion and in the manufacture of inorganic and semiconductor materials[1]. A range of electrochemical techniques is available[2–4] to characterise the mechanisms involved in copper electrochemistry and the process variables controlling electrode kinetics. The reduction of Cu(II) can be seen as two single-electron steps or as a single two-electron step, depending of the electrolyte composition. In particular, the presence of chloride ions stabilises the Cu(I) species, and the reaction Cu(II) to Cu(0) follows two single-electron steps[5,6], in contrast to the case in chloride-free, acid sulphate media[7].

The copper chloride electrolyte used in this investigation has a low cost and can be easily discharged to drain. For convenience, the experiments are carried out at room temperature. The stability of both Cu(II) and Cu(I) ions can be examined, providing clear insight into the understanding of the Cu(II) ion reduction mechanism and voltammetry as an electrochemical technique.

In chloride electrolytes, the reactions can be simplified to the reduction of Cu(II) – cupric – ions to Cu(I) – cuprous – ions (the latter being present as a dichlorocuprous anion.

$$Cu^{2+} + 2Cl^- + e^- \rightarrow CuCl_2^-. \quad (1)$$

Reaction (1) is followed by the reduction of Cu(I) ions to copper metal, *i.e.*, the deposition of copper.

$$CuCl_2^- + e^- \rightarrow Cu^0 + 2Cl^-. \quad (2)$$

The overall process for copper deposition from Cu(II) ions in chloride electrolyte is obtained by combining reactions (1) and (2).

$$Cu^{2+} + 2e^- \rightarrow Cu. \quad (3)$$

Under controlled conditions, it is possible to observe the forward and reverse reactions for electrode processes (1) and (2). In practice, this means selecting an appropriate range of electrode potential together with a suitable electrolyte composition and controlled flow conditions.

In this work, a cyclic voltammetry technique is used to demonstrate the reversibility of the Cu(II)/Cu(I) redox couple and the reversible, two stage reduction of Cu(II) to Cu(0) in acid (pHz) chloride. Steady state, linear sweep voltammetry at a rotating disc electrode is used to calculate the diffusion coefficients of Cu(II) and Cu(I) ions. The experiments demonstrate the use of simple electrochemical techniques and show how the deposition of copper can be carried out under controlled hydrodynamic conditions to provide general information on the electrochemistry of the system and to obtain kinetic data.

C. Ponce de Leon and F. C. Walsh, *Trans Inst Met Fin*, 2003, **81**(5), B11

Table I: Summary of experimental conditions.

Electrolyte	
Background electrolyte:	1.5 M NaCl at pH 2
Bulk reatant concentration, c:	0.0020M to 0.050M $CuCl_2$
Density, ρ	1.058 g cm^{-3}
Dynamic viscosity, η	0.0115 g cm^{-1} s^{-1}
Kinematic viscosity, $\nu=\eta/\rho$	0.0109 cm^2 s^{-1}
Temperature:	20°C (293 K)
Electrodes	
Working electrode:	Pt circular disc
WE surface:	Polished down to 0.3 microns on wet alumina
RDE radius, r	0.365 cm
RDE area, A	0.42 cm^2
Rotation speed (frequency, f'):	150 to 1870 rpm
Rotation speed (frequency, f'):	2.5 to 31.2 s^{-1}
Angular velocity ($\omega=2\pi f'/60$)	16 to 196 rad s^{-1}
Reference electrode:	Ag/AgCl/1M NaCl
Counter electrode:	Pt mesh (>5 cm^2 area)
Process conditions	
WE compartment volume:	100 cm^3
Potential sweep rate, dE/dt:	5 to 110 mV s^{-1}
Potentiostat:	HiTek 2 A/20V
Potential programmer:	HiTek PPR 101
x-y chart recorder:	PL3 (Seatallan Ltd)

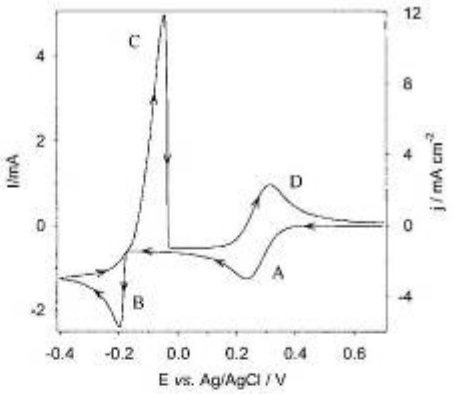

Figure 2. Cyclic voltammogram (current density vs. electrode potential), showing the general redox characteristics of 50mM $CuCl_2$ in 1.5M NaCl at 293 K. Potential limits: +0.70 V to −0.9 V vs. Ag/AgCl. Potential sweep rate = 5 mV s^{-1}. Pt RDE frequency = 0 s^{-1} (stationary disc electrode). Peak identification. 'A': Reduction of Cu(II) ions to Cu(I) ions, 'B': reduction of Cu(I) ions to Cu, 'C': oxidation of Cu to Cu(I) ions, 'D': Oxidation of Cu(I) ions to Cu(II) ions.

EXPERIMENTAL DETAILS

Table I shows the physical properties of the electrolyte together with details of the electrode areas, rotation rates and other experimental conditions. Figure 1 shows the electrochemical cell (within the experimental design set-up) used in the copper deposition experiments: the capacity of the cell is 100 cm^3 of electrolyte. The cell was constructed with a double wall to allow circulation of water maintaining the temperature of the electrolyte constant. The rotating disc electrode (working electrode) was inserted vertically into the electrolyte with its working surface facing the bottom of the cell. The silver/silver chloride reference electrode, placed in a separate compartment, contacted the bulk solution *via* a Luggin capillary, which was placed approximately 2 mm from the face of the working electrode. The counter (or auxiliary) electrode was placed in a compartment separated from the working electrolyte by a microporous glass frit. This arrangement avoided interference between products formed on the counter electrode and the working electrode. The counter electrode was a platinum mesh (*ca.* 2 cm^2) and a silver/silver chloride (ABB Instrumentation Ltd) reference electrode was used. All experiments were carried out at 293±1 K (20±1)°C.

Instrumentation used for voltammetry studies

Figure 1 also illustrates the electrical circuit. The potentiostat controlled the potential between the working and counter electrodes and allowed the current between the working and counter electrodes to be monitored. The potential and potential scan rates were controlled from the linear potential sweep unit. The current, I, was plotted against the potential of the working electrode, E (the latter being referred to the Ag/AgCl reference electrode). This resulted in an I-E curve of the type shown on the x-y chart recorder trace in Figure 1. The Hitek DT2101 potentiostat was controlled by a linear potential waveform generator (Hitek PPR1). The x-y recorder was a model PL3 from Seatallan Ltd. The rotating disc electrode rotator was an Oxford Instruments model capable of controlling rotation speed to within 1%.

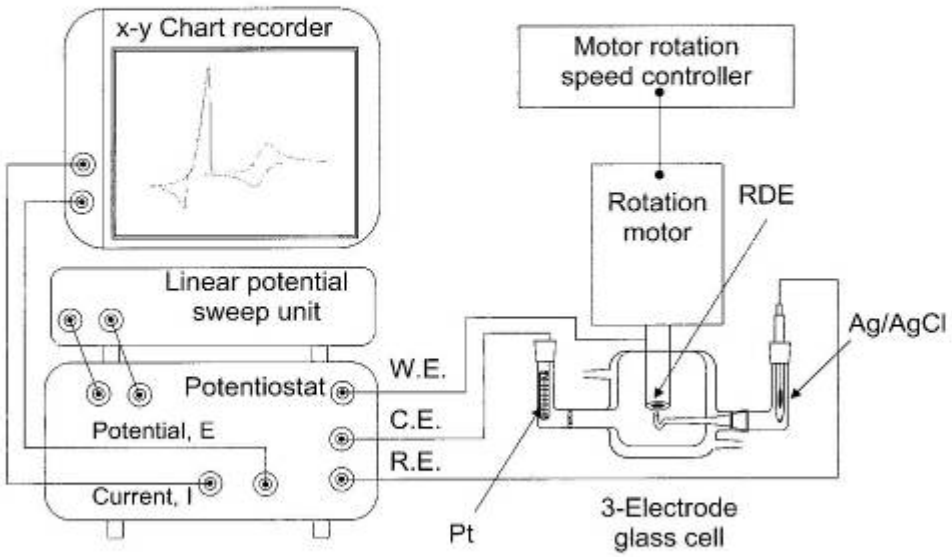

Figure 1. The instrumentation used for electrochemical voltammetry.

Experimental procedure

The supporting electrolyte consisted of 1.5 M NaCl at pH 2. Solutions with 2, 5, 10, 20 and 50 x 10^{-3} M of Cu(II) were prepared by dissolution of $CuCl_2$, followed by volumetric dilution. All of the reagents used were Analytical Reagent grade (Fisher Chemicals). Prior to each experiment, the working electrode (platinum disc) was manually polished with wet alumina powder on a polishing cloth, followed by rinsing with deionised water until its surface had a mirror finish. The solution was purged with a fast stream of dispersed nitrogen gas for 5 minutes before each experiment to avoid interference from the oxygen reduction reaction. The nitrogen supply was maintained over the surface of the electrolyte during the course of the experiments. In the cyclic voltammetry study of the redox couple Cu(II)/Cu(I), the potential range was from +0.70 to -0.16 V *vs.* Ag/AgCl (*all potentials quoted in this text are versus the silver/silver chloride reference electrode*) at a linear potential scan rate of 5 mV s^{-1}. In the rotating disc experiments the potential of the working electrode ranged from +0.70 to −0.60 V, at a scan rate of 10 mV s^{-1}.

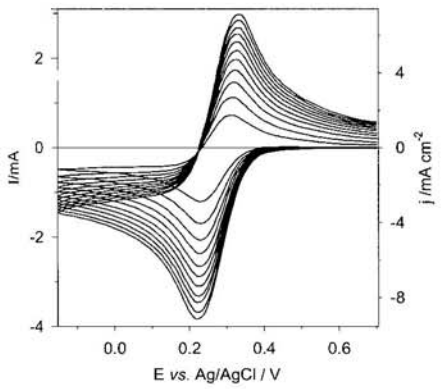

Figure 3. Cyclic voltammetry of the Cu(II)/Cu(I) couple (peaks 'A' and 'D' in Figure 2) in 50 mM $CuCl_2$ in 1.5M NaCl at 293 K, showing the effect of 10 mV s^{-1} potential sweep rate steps in the range 10 to 110 mV s^{-1}.

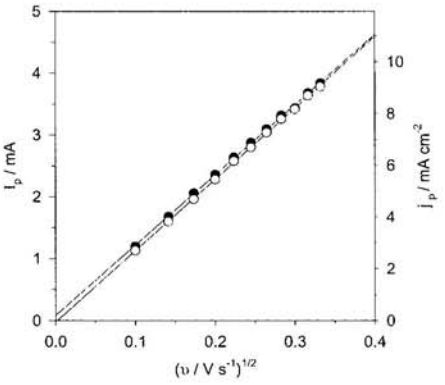

Figure 4. Randles-Sevčik (peak current vs. square root of potential sweep rate) plot for the Cu(II)/Cu(I) couple (analysis of the data in Figure 4). Electrolyte: 50 mM $CuCl_2$ in 1.5M NaCl at 293 K. Potential sweep rate: 10 to 110 mV s^{-1}.

RESULTS AND DISCUSSION

Cyclic voltammetry

Figure 2 shows a cyclic voltammogram for the reduction of 50 mM $CuCl_2$ in 1.5 M NaCl at pH 2 at a platinum electrode using a potential scan rate of 5 mV s^{-1}. The *I-E* curve shows several features. Peak 'A' represents the reduction of Cu(II) to Cu(I) commencing at 0.390 V with an approximate $E_{1/2}$ of 0.280 V. After reaching a maximum, the current decreases as the Cu(II) adjacent to the electrode surface has been consumed and new species from the bulk of the solution slowly diffuse towards the electrode.

As the potential becomes more negative, a peak 'B' commences at –0.17 V, corresponding to the reduction of Cu(I) to Cu(0). The shape of peak 'B' is characteristic of a phase change of the reactive species. In contrast to the reduction process in 'A' where the reduction product is soluble, the reduction of Cu(I) produces small nuclei of metallic copper attached to the electrode surface. These nuclei increase the area of the electrode producing a rapid steep increase in the current. After the peak, the current decreases in a similar manner to process 'A'.

During the reverse scan, a large anodic stripping peak 'C' is observed due to the dissolution of Cu(0) metal to Cu(I) ions. In contrast to processes 'A' and 'B', the Cu(0) reactant species in this case, is located on electrode surface and does not need to be transported, when the potential changes towards more positive values and metallic copper is no longer thermodynamically stable on the electrode surface the deposited copper dissolves back into the solution resulting in a drop in the observed current. It should be noted that the reverse and forward curves cross over the same potential value just before the dissolution of copper commences. In contrast to the case of carbon electrodes[2], there is no "nucleation loop" as the deposition of copper is thermodynamically favourable at negative potentials from this point due to the use of platinum as electrode material. In the case of electrode materials such as vitreous carbon, an overpotential of up to 0.2 V from the point in which the dissolution starts would be necessary to induce the formation of copper nuclei during the reduction process[2].

More positive potentials result in the oxidation of Cu(I) to Cu(II) represented by peak 'D'. After the maximum value, the current decreases in a similar manner to processes 'A' and 'B', due to the depletion of the reactive species on the electrode surface.

Figure 2 shows two electrochemical processes involving soluble/soluble species and two processes involving insoluble/soluble species, each process can be analysed independently by selecting the appropriate technique and potential range. The evaluation of the area under the curve for the deposition of copper, peak B, and the curve for the dissolution of copper, peak 'C', shows that, in both cases, the electrical charge q, was 0.0649 C, ($q_{dissolution}/q_{deposition} = 1$). During the deposition, the layer of copper on the electrode surface was visible, nevertheless, the concentration of the copper ions in solution remained practically constant as the thickness of the layer was 0.12 μm representing only 0.013% of the dissolved copper in the electrolyte solution. Hence, the bulk Cu(II) ion concentration can be considered to remain constant throughout the experiments.

Figure 3 shows a family of cyclic voltammograms for the redox process Cu(II)/Cu(I), corresponding to peaks 'A' and 'D' in Figure 2. The potential was swept from +0.70 V towards negative values and reversed at –0.16 V, avoiding the formation of metallic copper. The potential scan rate was controlled at values in the range 10 to 110 mV s^{-1} at 10 mV intervals. At low scan rates, the reduction product has more time to diffuse towards the bulk solution and the amount available for the oxidation is less resulting in a relatively smaller oxidising peak. The ratio between cathodic and anodic peak currents I_{pc}/I_{pa}, was approximately 0.95 at the lowest scan rate and approximates to 1 at the highest scan rate. A study of peaks 'A' and 'D' shows that both cathodic and anodic currents increase linearly with the square root of the sweep rate $v^{1/2}$, according to the Randles-Sevčik equation,

$$I_p = 2.69 \times 10^5 z^{3/2} A D^{1/2} v^{1/2} c \qquad (4)$$

as shown in Figure 4. I_p is the peak current, z the number of electrons, A the electrode area, D the diffusion coefficient, v the potential scan rate and c the concentration. The diffusion coefficients for Cu^{2+} and $CuCl_2^-$ species calculated from the slopes of the curves from Figure 4, *via* equation (4), were (4.2 ± 0.2) x 10^{-6} and (4.3 ± 0.2) x 10^{-6} cm^2 s^{-1}. These were obtained using the cathodic and anodic

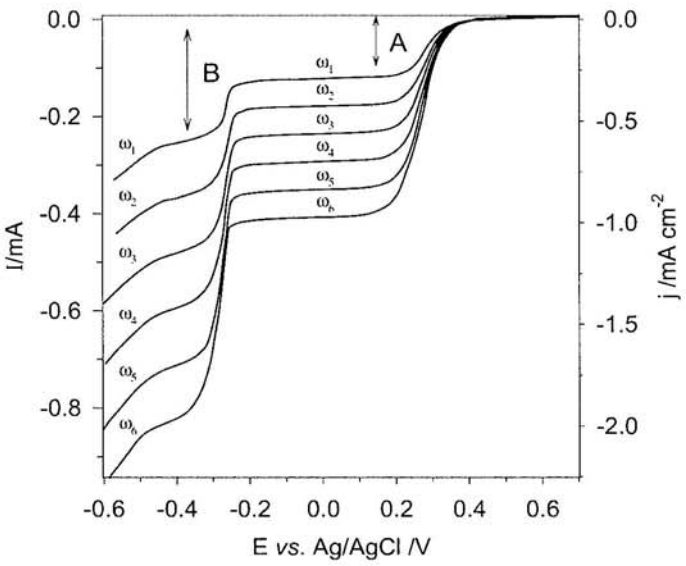

Figure 5. The effect of rotation frequency (2.5 to 31.2 s^{-1}) of the rotating disc electrode on the linear sweep voltammetry (current vs. electrode potential) of 'A': Cu(II) reduction to Cu(I) ions then 'B': Cu(I) reduction to Cu in 1.5M NaCl containing 2 mM $CuCl_2$ at 293 K is shown. Potential sweep rate: 10 mV s^{-1}. ω_1 = 16, ω_2 = 36, ω_3 = 64, ω_4 = 100, ω_5 = 144, and ω_6 = 196 rad s^{-1}. (ω_1 =152, ω_2 =343, ω_3 =610, ω_4 =954, ω_5 =1375 and ω_6 =1870 rpm).

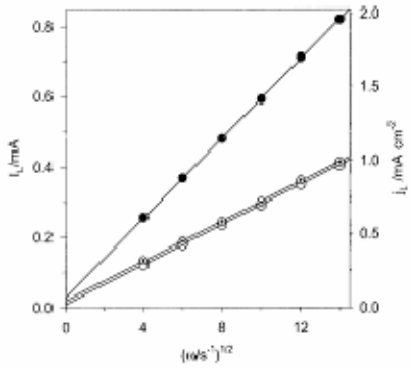

Figure 6. Levich (limiting current vs. square root of angular velocity) plot for the rotating disc electrode data shown in Figure 5. ○ plateau 'A', ● plateau 'B' in Figure 6, ⊙ 'B minus A.

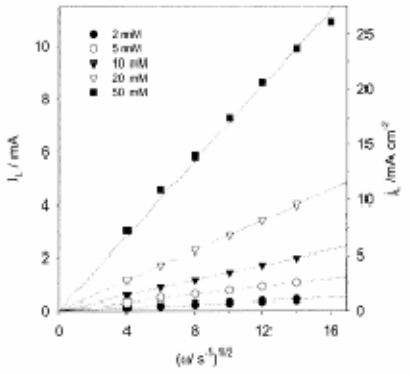

Figure 7. Levich plots for the reduction of Cu(II) to Cu(I) ions in 1.5M NaCl containing 2 mM to 50 mM $CuCl_2^-$ at 293 K. RDE frequency: 2.5-31.2 s^{-1}. Potential sweep rate: 10 mV s^{-1}.

branches, respectively and are reported in Appendix 2 where they are compared with data obtained as detailed in the following section.

Cyclic voltammetry at a rotating disc electrode

Figure 5 shows a typical family of *I-E* curves for the reduction of 2 mM Cu(II) to Cu(0) at rotation frequencies from 150 to 1870 rpm (2.5 to 31.2 Hz; 16-192 rad s^{-1}), the potential was scanned from +0.70 to −0.60 V at a scan rate of 10 mV s^{-1}. For the lowest rotation rate, 150 rpm, ($\omega^{1/2} = 4$ (rad s^{-1})$^{0.5}$), the reduction of Cu(II) ions to Cu(I) ions, process 'A', starts at approximately the same potential as in the cyclic voltammogram shown in Figure 2. The reduction process is observed as a constant current plateau region rather than a peak, since the continuous rotation of the electrode maintains a constant supply of Cu(II) ions to the surface of the disc.

As the electrode potential becomes more negative, the reduction of Cu(I), process 'B', appears at a potential of approximately -0.24 V. Cu(I) species on the electrode surface are reduced to Cu(0), generating another plateau region, which is less well defined as it is affected by a secondary reaction, hydrogen evolution. It should be noted that at this potential the processes A and B take place at the same time, the rotation of the electrode brings Cu(II) ions from the bulk of the solution to the electrode surface which is immediately reduced to Cu(I) ions and then to Cu(0) metal. Under such conditions, the reduction of Cu(II) ions appears as a single step of two electrons and the current of the step B of Figure 5 is approximately twice the size of the current in process 'A'. The two plateaux regions are characterised by a limiting current value, which is proportional to the rate at which the reactant species reach the electrode surface. Under these conditions the reaction rate is limited by the rate of mass transport and the limiting current value can be predicted by the Levich equation,

$$I_L = 0.620\, z\, FAD^{2/3}\omega^{1/2}\nu^{-1/6}c \qquad (5)$$

where I_L is the limiting current, F the Faraday constant, ω the rotation rate and ν the kinematic viscosity of the electrolyte. At higher rotation frequencies, ω >150 rpm; $\omega^{1/2} > 4$ (rad s^{-1})$^{0.5}$, the *I-E* curves have a similar shape and the supply of electroactive species to the electrode surface is faster resulting in higher limiting currents; the stagnant diffusion layer adjacent to the electrode surface reduces its thickness as the rotation rate increases. Figure 6 shows the limiting current values plotted against $\omega^{1/2}$ for the process 'A', 'B' and 'A minus B' from Figure 5, where A corresponds to the reduction of Cu(II) ions to Cu(I) ions, B corresponds to the total current of the reduction of Cu(II) ions to Cu(0) metal, which appears as one single step of two electrons and 'A minus B' corresponds to the current for the process Cu(I) to Cu(0). The linear correlation between I_L and $\omega^{1/2}$ shows that in these reduction processes the mechanisms are mass transport controlled. Similar curves to those presented in Figure 5 were obtained for concentrations of 5, 10, 20 and 50 x 10^{-3} M Cu(II) and their corresponding plot of I_L *vs.* $\omega^{1/2}$ shows that they are completely mass transport controlled.

The diffusion coefficient values for Cu^{2+} and the $CuCl_2^-$ ion obtained from cyclic voltammetry at a stationary disc electrode and from linear sweep voltammetry at a rotating disc electrode for species are comparable. Table II lists the diffusion coefficient values for $CuCl_2^-$ and Cu^{2+} species determined by electrochemical techniques both from this work and from the literature. The majority of the literature *D* values for $CuCl_2^-$ in aqueous chloride media near room temperature are in the range of (4.1 – 10) x 10^{-6} cm^2 s^{-1} [19-22], in agreement with the values obtained in the present work. Electroanalytical literature cited in the past has contained values for diffusion coefficients, as high as (14.2 x 10^{-6} cm^2 s^{-1})[8-14] The diffusion coefficients values for Cu^{2+} from this work and from the literature are within the range (4.1 – 7.4) x 10^{-6} cm^2 s^{-1} [2,5,8-9,14,18].

Effect of Cu(II) concentration and electrode rotation frequency on the limiting current

Figure 7 shows curves of I_L *vs.* $\omega^{1/2}$ for the reduction of Cu(II) to Cu(I) at different Cu(II) concentrations. The limiting currents increase proportionally to the concentration. For example, at constant rotation frequency of $\omega^{1/2} = 4$ Hz$^{0.5}$, the limiting current of a 50 mM solution is 10 times the limiting current in a 5mM solution.

Similarly, Figure 8 shows a family of curves of I_L *vs. c* for the reduction of Cu(II) to Cu(I)

Table II: Diffusion coefficients for Cu(II) and Cu(I) ions.

$D_{Cu(II)}$ /10^{-6} cm^2 s^{-1}	$D_{Cu(I)}$ /10^{-6} cm^2 s^{-1}	Electrolyte conditions, technique etc.	Ref.
4.1 ± 0.2	4.2 ± 0.2	Cyclic voltammetry (Figure 3), Pt, 293K	This work
4.3 ± 0.2	4.5 ± 0.2	Steady state RDE linear sweep voltammetry, Pt, 293 K	
5.6		5 mM Cu(II) in 1.5 M NaCl, carbon electrode	2
5.3		RDE, 10 mM CuSO4 in 0.5 Na_2SO_4, pH 2.0, Pt, 298 K.	5
7.4	11.8	2.51M Cu(II)/Cu(I) in 1M KBr + 10^{-2} M H_2SO_4, 298 K	8
5.7		Cu(II)/Cu(I) in 0.2M H_2SO_4, 298 K	8
6		0.8 M Na_2SO_4, pH 2.5	9
7.5 ± 0.01	14.2 ± 0.06	Chronopotentiometry Cu(II)/Cu(I) 2.47 x 10^{-2} M, 1M HCl, 298 K	14
7.8 ± 0.01	13.3 ± 0.05	Chronopotentiometry Cu(II)/Cu(I) 2.03 x 10^{-2} M, 1M KCl, 298 K	14
7.35 ± 0.18		RDE and Chronopotentiometry, $CuSO_4$ infinite dilution, 0.5M H_2SO_4, 298 K	18
5.5		$CuCl_2$ 0.1 to 1.0M NaCl at 296 ± 1 K	19
5.4		$CuCl_2$ 0.1 to 2.0M HCl at 298 K	20
10		$CuCl_2$ 0.5 to 3M in xM HCl at 298 K	21
5		$CuCl_2$ see water 298 K	22

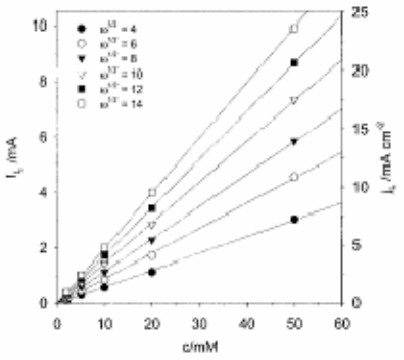

Figure 8. Limiting current vs. Cu(II) concentration for the reduction of Cu(II) to Cu(I) ions in 1.5M NaCl containing 2-50 mM $CuCl_2$ at 293 K. RDE frequency: 2.5-31.2 s^{-1}. Potential sweep rate: 10 mV s^{-1}.

ions at a series of rotation frequencies. The slope of the curves increases with the rotation rate. The relationship between the limiting current and concentration can be expressed as,

$$I_L = k_m AzFc \qquad (6)$$

where, k_m is the mass transport coefficient. Appendix 2 shows the slopes of the curves of Figure 8 and the values of the mass transport coefficients calculated for the reduction of Cu(II) ions to Cu(I) ions and Cu(I) ions to metallic Cu(0). At low rotation frequencies, the mass transport coefficient in both processes is the same. However, at higher rotation frequencies, the mass transport coefficient is higher for the reduction of Cu(I) ions to Cu(0) metal, the increase is attributable to the increased area of the electrode due to the formation of roughened copper deposits.

CONCLUSIONS

The voltammetric experiments show that the first step in the reduction of Cu(II) ions to Cu(I) ions is a reversible process and follows the Randles-Sevčik equation. The stabilisation of Cu(I) in chloride media allows the observation of the reduction of Cu(II) to Cu(I) ions (and the reverse process) in rotating disc electrode experiments. The reduction current follows the Levich equation, indicating that the processes are mass transport controlled. The diffusion coefficients calculated from cyclic voltammetry at a stationary disc and from rotating disc electrode techniques are similar for Cu(II) ions. The values of the diffusion coefficients calculated here are comparable to those reported in the literature although reported diffusion coefficients vary over a large range depending on the authors and the experimental conditions. The amount of electroactive species deposited during the reduction of Cu(I) to Cu(0) was negligible in comparison with the concentration of the bulk solution. The use of a platinum electrode shows that there is no need to impose an overpotential on the electrode, in order to deposit Cu(0), as a result no nucleation loop is observed as in the case of other electrode materials, such as vitreous carbon[8].

ACKNOWLEDGEMENTS

The authors are grateful to Professor Derek Pletcher (University of Southampton) for early discussions on the electrochemistry of Cu(II)/(I) in chloride electrolytes.

List of Symbols

Symbol	*Meaning*	*Units*
A	RDE area ($=\pi r^2$)	cm^2
c	Bulk reactant concentration	mol cm^{-3}
D	Diffusion coefficient	cm^2 s^{-1}
E	Electrode potential (*vs.* Ag/AgCl)	V
F	Faraday constant (=96 485 C mol^{-1})	C mol^{-1}
I	Current	A
I_p	Peak current (in cyclic voltammogram)	A
j	Current density	A cm^{-2}
k_m	Mass transport coefficient	cm s^{-1}
r	Radius of rotating disc electrode	cm
z	Number of electrons	–
ω	Rotation rate of RDE	rad s^{-1}
ν	Kinematic viscosity of electrolyte	cm^2 s^{-1}

REFERENCES

1. D. Pletcher and F.C. Walsh, *"Industrial Electrochemistry"*, 2nd Edition, Blackies, Bishopbriggs, UK, 1990.
2. D. Pletcher, *"A First Course in Electrode Processes"*, The Electrochemical Consultancy, Romsey, 1991.
3. F.C. Walsh, *"A First Course in Electrochemical Engineering"*, The Electrochemical Consultancy, Romsey, 1993.
4. D. Pletcher, R. Greef, R. Peat, L.M. Peter and J. Robinson, *"Instrumental Methods in Electrochemistry"*, Horwood Publishing Ltd, Chichester, 1985; reprinted 2001.
5. G. Kear, B.D. Barker and F.C. Walsh, *Corr. Sci.*, 2003, in the press.
6. J.R. Smith, S.A. Campbell and F.C. Walsh, *Trans. Inst. Metal Fin.*, 1995, **73**(2), 72.
7. E. Man, E.E. Farndon, S.A. Campbell and F.C. Walsh, *Trans. Inst. Metal Fin.*, 1996, **74**(1), 39.
8. U. Bertocci and D. Turner *in "Encyclopaedia of the Electrochemistry of the Elements"*, Vol. II, Ed. A. J. Bard, Marcel Dekker, 1973.
9. D. Bennion and J. Newman, *J. Appl. Electrochem.*, 1972, **2**, 113.
10. A.J. Bard & L.R. Faulkner, *Electrochemical Methods*, Wiley, New York, 1980.
11. A.J. Bard & L.R. Faulkner, *"Electrochemical Methods. Fundamentals and Applications"* 2nd Edition, Wiley, Chichester, 2001.
12. C. Brett and O. Brett *"Electrochemistry: Principles, Methods, and Applications"*, Oxford University Press, Oxford, 1998.
13. A.C. Fisher *"Electrode Dynamics"*, Oxford University Press, Oxford, 1996.
14. D. J. Peters, and S. A. Cruser, *J. Electroanal. Chem.*, 1965, **9**, 27.
15. D. T. T. Napp, D. C. Johnson and S. Bruckenstein, *Anal. Chem.*, 1939, **39**(4), 481.
16. B. Miller and M. I. Bellavance, *J. Electrochem. Soc.*, 1972, **119**(11), 1510.
17. A. J. deBethune, T. S. Licht and N. Swendeman, *J. Electrochem. Soc.*, 1959, **169**(7), 616.
18. T. I. Quickenden and X. Jiang, *Electrochim. Acta*, 1984, **29**(6), 693.
19. F. King, C. D. Litke, M. J. Quin, and D. M. LeNeveu, *Corr. Sci.*, 1995, **37**, 833.
20. B. Tribollet and J. Newman, *J. Electrochem. Soc.*, 1984, **131**, 2780.
21. A. Moreau, *Electrochim. Acta*, 1981, **26**, 497.
22. R. J. K. Wood, S. P. Hutton, and D. J. Schiffrin, *Corr. Sci.*, 1990, 30, 1177.

Appendix 1: *Tables of Voltammetry Data*

'A' (corresponding to Figure 7): Cu(II) → Cu(I)

$(\omega$/rad s$^{-1})^{1/2}$	Limiting current/mA				
	2mM	5mM	10mM	20mM	50mM
4.0	0.122	0.305	0.58	1.14	3.04
6.0	0.180	0.460	0.87	1.72	4.56
8.0	0.236	0.605	1.14	2.28	5.84
10.0	0.292	0.750	1.43	2.86	7.32
12.0	0.350	0.895	1.72	3.42	8.64
14.0	0.406	1.045	2.00	4.00	9.90
16.0					10.95

'B' (corresponding to Figure 8): Cu(II) → Cu(0)

$(\omega$/rad s$^{-1})^{1/2}$	Limiting current/mA				
	2mM	5mM	10mM	20mM	50mM
4.0	0.256	0.610	1.190	2.30	6.04
6.0	0.368	0.915	1.730	3.46	9.06
8.0	0.480	1.210	2.300	4.58	11.92
10.0	0.592	1.500	2.900	5.78	14.80
12.0	0.712	1.800	3.470	6.92	17.68
14.0	0.820	2.095	4.045	8.08	20.40
16.0					22.40

'B minus A' (by calculation): Cu(I) → Cu(0)

$(\omega$/rad s$^{-1})^{1/2}$	Limiting current/mA				
	2mM	5mM	10mM	20mM	50mM
4.0	0.134	0.305	0.610	1.16	3.00
6.0	0.188	0.455	0.860	1.74	4.50
8.0	0.244	0.605	1.160	2.30	6.08
10.0	0.300	0.750	1.470	2.92	7.48
12.0	0.362	0.905	1.750	3.50	9.04
14.0	0.414	1.050	2.045	4.08	10.50
16.0					11.45

Appendix 2: *Specimen Calculations*

Diffusion coefficient of Cu(II) ions from cyclic voltammetry at a stationary disc electrode, using the Randles-Sevčik equation.

Slope of cathodic I_p *vs.* $v^{1/2}$ = 0.01136 A V$^{-1/2}$ s$^{1/2}$
Cathodic: $D_{Cu(II)}$ = (4.1 ± 0.2) x 10^{-6} cm^2 s^{-1}
Anodic: $D_{Cu(II)}$ = (4.2 ± 0.2) x 10^{-6} cm^2 s^{-1}

Diffusion coefficient of Cu(II) ions from linear sweep voltammetry at an RDE using the Levich equation.

[Cu(II)] /mM	$D_{Cu(II)/Cu(I)}$ / 10^{-6} cm^2 s^{-1}	$D_{Cu(II)/Cu(0)}$ / 10^{-6} cm^2 s^{-1}	$D_{Cu(I)/Cu(0)}$ / 10^{-6} cm^2 s^{-1}
	'A'	'B'	'B minus A'
2	4.3±0.2	4.3±0.2	4.3±0.2
5	4.6±0.2	4.6±0.2	4.7±0.2
10	4.4±0.2	4.4 ±0.2	4.5±0.2
20	4.4±0.2	4.5±0.2	4.5±0.2
50	3.9±0.2	4.2±0.2	4.5±0.2

Mass transport coefficient for Cu(II) reduction from limiting current *vs.* concentration plot of linear sweep voltammetry data at an RDE.

f/rev min^{-1}	ω/rad s^{-1}	ω/rad s$^{-1})^{1/2}$	Cu(II) → Cu(I) Slope of I_L vs. c /A mol^{-1} cm^3	Cu(II) → Cu(I) k_m /10^{-3} cm s^{-1}	Cu(I) → Cu(0) Slope of I_L vs. c /A mol^{-1} cm^3	Cu(I) → Cu(0) k_m /10^{-3} cm s^{-1}
153	16	4	60.2	1.5	59.7	1.5
344	36	6	90.4	2.2	90.0	2.2
611	64	8	116.4	2.9	121.7	3.0
955	100	10	145.9	3.6	149.6	3.7
1375	144	12	172.6	4.3	180.9	4.5
1490	156	14	198.4	4.9	210.1	5.2